

# Brivaracetam Differentially Affects Voltage-Gated Sodium Currents Without Impairing Sustained Repetitive Firing in Neurons

Isabelle Niespodziany, Véronique Marie André, Nathalie Leclère, Etienne Hanon, Philippe Ghisdal & Christian Wolff

UCB Pharma SA, Neurosciences Therapeutic Area, Braine l'Alleud, Belgium

## Keywords

Action potential firing; Antiepileptic drug; Neurons; Voltage-gated sodium channel.

## Correspondence

Isabelle Niespodziany, UCB Pharma SA, East-R1 Building, Chemin du Foriest, B-1420 Braine l'Alleud, Belgium.

Tel: +32-2-386-2643;

Fax: +32-2-386-3397;

E-mail: isabelle.niespodziany@ucb.com

Received 25 July 2014; revision 3 October

2014; accepted 5 October 2014

doi: 10.1111/cns.12347

## SUMMARY

**Aims:** Brivaracetam (BRV) is an antiepileptic drug in Phase III clinical development. BRV binds to synaptic vesicle 2A (SV2A) protein and is also suggested to inhibit voltage-gated sodium channels (VGSCs). To evaluate whether the effect of BRV on VGSCs represents a relevant mechanism participating in its antiepileptic properties, we explored the pharmacology of BRV on VGSCs in different cell systems and tested its efficacy at reducing the sustained repetitive firing (SRF). **Methods:** Brivaracetam investigations on the voltage-gated sodium current ( $I_{Na}$ ) were performed in N1E-155 neuroblastoma cells, cultured rat cortical neurons, and adult mouse CA1 neurons. SRF was measured in cultured cortical neurons and in CA1 neurons. All BRV (100–300  $\mu$ M) experiments were performed in comparison with 100  $\mu$ M carbamazepine (CBZ). **Results:** Brivaracetam and CBZ reduced  $I_{Na}$  in N1E-115 cells (30% and 40%, respectively) and primary cortical neurons (21% and 47%, respectively) by modulating the fast-inactivated state of VGSCs. BRV, in contrast to CBZ, did not affect  $I_{Na}$  in CA1 neurons and SRF in cortical and CA1 neurons. CBZ consistently inhibited neuronal SRF by 75–93%. **Conclusions:** The lack of effect of BRV on SRF in neurons suggests that the reported inhibition of BRV on VGSC currents does not contribute to its antiepileptic properties.

## Introduction

Brivaracetam (BRV) is an antiepileptic drug (AED) currently in Phase III clinical development for the add-on treatment of refractory partial-onset seizures in adults. BRV provided a positive outcome in Phase IIa trials where the drug showed high efficacy in patients suffering from photosensitive epilepsy [1] and in Phase IIb trials where BRV demonstrated efficacy and high tolerability as an adjunctive treatment in adult patients with refractory partial-onset epilepsy [2,3]. More recent results from Phase III studies reported that adjunctive BRV showed efficacy and good tolerability in adults with uncontrolled partial-onset and generalized epilepsies [4–6].

Brivaracetam was developed by a rational drug discovery approach [7] following the discovery of levetiracetam (LEV, Keppra<sup>®</sup>), a drug with a novel molecular mode of action characterized by binding to synaptic vesicle protein 2A (SV2A) [8]. BRV has a 20-fold higher affinity than LEV in binding to the native or recombinant SV2A protein [9], which translates to increased potency in different seizure models [10]. BRV is also distinct from LEV by its ability to protect against seizures in normal mice induced by a maximal electroshock or maximal

dose of pentylenetetrazol [10], while LEV had no effect in those models, and by a more potent and complete seizure suppression in kindled animals. This corroborates *in vitro* studies showing that BRV has higher potency and efficacy than LEV against epileptiform responses in two different *in vitro* rat hippocampal slice models of epilepsy in a dose range which is relevant for its clinical efficacy [1,10,11]. The significant correlation between the kinetics of *in vivo* SV2A occupancy and seizure protection [9] supports the hypothesis that BRV reduces neuronal hyperexcitability by modulating synaptic release through a mechanism similar to the one described for LEV [12,13].

Levetiracetam is believed to primarily exert its antiepileptic activity through a unique mechanism of action involving binding to the SV2A protein [8,14], although other mechanisms including actions on voltage-gated calcium channels [15,16], and AMPA and GABA<sub>A</sub> receptors [17] may potentially contribute to its anti-convulsant properties. In contrast to LEV [18], BRV has been shown to inhibit voltage-gated sodium channels (VGSC) in primary cortical cultures [19]. Similar to classical AEDs acting on VGSC, BRV modulates the inactivated state of the channels, shifts the voltage dependence of inactivation to more hyperpolarized potentials ( $K_I$  of 7.7  $\mu$ M), and significantly delays the recovery

from fast inactivation. BRV was also reported to modulate VGSC in the resting state ( $K_R$  of 41  $\mu$ M), an effect which is not observed with classical AEDs [20,21]. Inhibition of VGSCs translates into reduced action potential (AP) firing and neurotransmitter release and represents one of the major mechanism of AEDs to reduce hyperexcitability of neuronal networks [22] and to produce anti-convulsant activity [23]. BRV reduces epileptiform activity *in vitro* [10] but so far no data are available on its effects on the intrinsic firing activity in neurons. Based on the recent findings that BRV modulates VGSCs, we hypothesized that BRV was able to reduce sustained repetitive firing (SRF) *in vitro*. In this study, we extended the previous observations by Zona *et al.* [19] by studying the pharmacology of BRV in comparison with carbamazepine (CBZ), on VGSCs expressed in neuroblastoma N1E-115 cells, in rat cultured cortical neurons, and in CA1 neurons from mouse hippocampal slice. To further understand whether the effect of BRV on VGSCs translates into inhibition of neuronal excitability, we also investigated and compared the effect of BRV and CBZ on the SRF. Altogether, these experiments should allow us to validate whether the effect of BRV on VGSCs represents a relevant mechanism that contributes to its antiepileptic properties.

## Materials and Methods

### Ethics Statement

All animals were treated in accordance with the declaration of Helsinki and following the guidelines of the Belgium Ministry of Agriculture. Experiments from animals were approved by Ethics Committee of UCB Pharma SA.

### N1E-115 Neuroblastoma Cells

N1E-115 mouse neuroblastoma cells (ATCC<sup>®</sup> CRL-2263<sup>TM</sup>) were subcultured and grown on glass coverslips in Dulbecco's modified Eagle's medium containing 9% fetal bovine serum and 5000 U penicillin/streptomycin (cell density 20,000–40,000 cells/ml). Cells were incubated at 37°C with 5% CO<sub>2</sub> in 35 mm culture dishes and were used for electrophysiological experiments 24–48 h after plating.

### Primary Culture of Rat Cortical Neurons

Neocortex was removed from E17–E18 Wistar embryonic rats, dissociated in 0.25% trypsin (Invitrogen), and triturated in complete neurobasal-based medium composed of neurobasal medium (Invitrogen), 10% horse serum (Lonza), 2% B27 serum-free supplement (Invitrogen, Carlsbad, CA, USA), 0.5 mM glutamax (Invitrogen), and 1% penicillin/streptomycin (Lonza, Verviers, Belgium). Coverslips coated with poly-D-lysine (Sigma, St. Louis, MO, USA) and laminin (Sigma) were then seeded, and neurons (40,000–50,000 cells/ml) were grown in complete neurobasal-based medium.

### Hippocampal Slices from Adult Mouse

Hippocampal slices were prepared from male C57 black mice (Charles River Laboratories). Mice were 8–10 weeks old for

SRF study and 4 weeks old for  $I_{Na}$  study. Animals used for  $I_{Na}$  recordings were younger to improve the number of healthy neurons at the slice surface, to help to perform successful patch-clamp recordings. On the day of the experiment, the mouse was deeply anesthetized with isoflurane and rapidly decapitated. The brain was quickly removed and placed in an oxygenated (95% O<sub>2</sub>/5% CO<sub>2</sub>) modified ice-cold artificial cerebrospinal fluid (mACSF) composed of (in mM) choline chloride 126, KCl 3, CaCl<sub>2</sub> 2.4, MgCl<sub>2</sub> 1.3, NaH<sub>2</sub>PO<sub>4</sub> 1.24, NaHCO<sub>3</sub> 26, glucose 10, pH 7.3. Sagittal slices (250–350  $\mu$ m-thick) containing hippocampus were prepared according to standard procedures with a vibratome (Leica VT1000S type) and kept either at 30°C or at room temperature in oxygenated (95% O<sub>2</sub>/5% CO<sub>2</sub>) standard ACSF containing (in mM): NaCl 126, KCl 3, CaCl<sub>2</sub> 2.4, MgCl<sub>2</sub> 1.3, NaH<sub>2</sub>PO<sub>4</sub> 1.24, NaHCO<sub>3</sub> 26, glucose 10, pH 7.3.

## Electrophysiological Recordings

All recordings were performed in tight-seal, whole-cell patch-clamp configuration excepted for SRF experiments in CA1 neurons which were performed with intracellular recordings using sharp microelectrodes. Intracellular sharp microelectrodes were pulled from 1.0-mm (inside diameter) borosilicate glass capillaries (Hilgenberg) and had an impedance of 100–200 M $\Omega$  after filling with KCl 3 M. Patch pipettes were pulled from 1.5-mm (inside diameter) borosilicate glass capillaries (Harvard) and had a resistance of 4–5 M $\Omega$  when filled with intracellular solution. Neuroblastoma cells and primary cortical neurons were visualized with an inverted microscope (IX71; Olympus), while slices were visualized with infrared differential interference contrast video microscopy on an upright microscope (BX50; Olympus Europa Holding GmbH, Hamburg, Germany) or with a standard binocular stereomicroscope (Stemi; Zeiss, Oberkochen, Germany). Data were recorded at room temperature (20–22°C) for all experiments excepted for SRF study in CA1 neurons performed at 32°C. All preparations were continuously perfused with oxygenated extracellular (EC) solution at a rate of ~1 ml/min. For whole-cell experiments, the junction potential (JP) between the recording pipette and the extracellular solution was measured (see JP values in Solution and Drugs part) and compensated for by on-line subtraction. For voltage-clamp recordings, series resistances were compensated by 70–90% on the amplifier (Axopatch 200B or Multiclamp 700B; Molecular Devices, Sunnyvale, CA, USA). After seal formation, the pipette capacitive current was cancelled, and following break through, the whole-cell capacitive current was cancelled. On-line leak subtraction was performed using a P/4 protocol. For current-clamp recordings using whole-cell configuration and intracellular recordings, pipette capacitance neutralization and bridge balance were set through the amplifier (Axopatch 200B or Axoclamp 2B; Molecular Devices). Currents and potentials were filtered at 10 kHz and digitized at 20 kHz using a Digidata 1322A converter and the acquisition program pClamp (Molecular Devices).

Detailed experiments and protocols for induction of  $I_{Na}$  and SRF in the different investigated cell systems are described in Data S1.

## Solutions and Drugs

In N1E-115 cells, for  $I_{Na}$  recordings, the compositions of intracellular solution (IC) and EC were similar to those previously reported [24] with a JP of 6 mV. In cortical primary neurons, for  $I_{Na}$  recordings, IC was composed of (in mM) CsF 110, NaCl 15,  $CaCl_2$  1, TEA-Cl 10, EGTA 10, HEPES 10, ATP-Mg 4, GTP-Tris 0.3, leupeptin 0.1, phosphocreatine 10, pH 7.2, 290 mOsm/l. EC was modified to induce smaller  $I_{Na}$ , easier to clamp and was composed of (in mM) NaCl 80, choline-Cl 40, TEA-Cl 15,  $MgCl_2$  2,  $CaCl_2$  1, HEPES 10, glucose 20, 4-AP 2,  $CdCl_2$  0.2, sucrose 10, pH 7.4, 300 mOsm/l, JP with respective IC was 8 mV. For SRF recordings in current-clamp, IC was composed of (in mM) K-gluconate 110, KCl 20, HEPES 10, phosphocreatine-diNa 10,  $MgCl_2$  2, diNa-ATP 2, EGTA 1, GTP-Tris 0.25, pH 7.3, 290 mOsm/l. EC was composed of (in mM) NaCl 142, D-glucose 20, HEPES 10, NBQX 10, KCl 2.5,  $CaCl_2$  2,  $MgCl_2$  1, pH 7.4, 315 mOsm/l, JP with respective IC was 15 mV. In mouse hippocampal slices, for  $I_{Na}$  recordings, IC was composed of (in mM): CsF 110, NaCl 15, EGTA 10, HEPES 10,  $CaCl_2$  1,  $MgCl_2$  2, TEA-Cl 10, ATP-Mg 2, pH 7.3, 300 mOsm/l. EC was composed of (in mM): NaCl 63, choline-Cl 63, KCl 3, TEA-Cl 20,  $MgCl_2$  1.3,  $CaCl_2$  2.4, TRIS 25, 4-AP 2,  $CoCl_2$  2.5, glucose 10, pH 7.3, 310 mOsm/l, JP with respective IC was 7 mV. For SRF recordings in current-clamp, EC was composed of standard ACSF. All tested compounds were dissolved in dimethylsulfoxide (DMSO) to make stock solutions. The final concentration of DMSO in the extracellular solution was 0.1–0.2% (v/v) for brivacetam (BRV; UCB Pharma SA, Braine l'Alleud) and carbamazepine (CBZ; Sigma). Control groups perfused with drug-free solutions contained equal concentrations of DMSO.

## Data Analysis and Statistics

Values of  $I_{Na}$  were plotted on a graph as a function of the step potential to generate I–V curves, and mean values for activation threshold, maximal current amplitude, and peak potential were measured. To build fast inactivation curves,  $I_{Na}$  amplitude activated by the final test pulse was measured at the peak current, normalized according to the maximal  $I_{Na}$ , and plotted according to the preconditioning step values. The inactivation curve was fitted with the following Boltzmann equation:  $I/I_{max} = 1/[1 + \exp[(V - V_{50})/k]]$ , where  $I_{max}$  is the peak current,  $V_{50}$  is the voltage at which half-maximum current occurs,  $V$  is the test potential, and  $k$  is the slope factor. In N1E-115 cells, we observed no rundown or runup of  $I_{Na}$  during the 1 Hz pulse-protocol, thus we did not record a control group for time. We measured the effect of the drugs on  $I_{Na}$  recorded from resting state or inactivated state of VGSCs by normalizing the smallest  $I_{Na}$  value recorded during the 3-min drug perfusion to the mean of the last 6 data points recorded in control conditions (baseline). In primary cortical and CA1 neurons, we observed a rundown of 0.1 Hz pulse-generated  $I_{Na}$  when induced from VGSCs inactivated state. Therefore, we also recorded a untreated control group to compare with drug-treated groups. The effect of the drugs on  $I_{Na}$ , time course was analyzed with a linear biregression fit before and after perfusion of the drug. Thus, drug effect was calculated at the time of the solution change, as the difference between the extrapolation of the straight line measured during perfusion with control EC solution

and the straight line measured during drug perfusion. To measure drug effect on SRF in primary cortical neurons, the number of APs evoked per depolarizing step was counted every 5 min and normalized to the number of APs elicited before drug application or time match control. The time course of APs number percentage was plotted for each group of neurons. To evaluate drug effect on SRF in CA1 neurons, the number of APs elicited per series of depolarizing steps was counted every 10 min. Statistical analyses were performed using unpaired two-tailed *t*-test or one-way ANOVA followed by a post hoc LSD test to compare each drug-treated group with the corresponding control group ( $*P < 0.05$ ;  $*P < 0.01$ ;  $***P < 0.001$ ) or using paired two-tailed *t*-test to compare postdrug to predrug parameter in the same group ( $*P < 0.05$ ;  $*P < 0.01$ ;  $***P < 0.001$ ).

## Results

### In N1E-115 Cells, BRV Shifts the Voltage Dependence of $I_{Na}$ Fast Inactivation to More Hyperpolarized Potentials and Reduces $I_{Na}$ When VGSCs are in an Inactivated State

The effects of BRV and of CBZ on  $I_{Na}$  were investigated in a first series of experiments performed in N1E-115 cell line (Figure 1) that we previously demonstrated to express tetrodotoxin-sensitive VGSCs [24]. The stimulation protocol illustrated in Figure 1A was utilized to assess the effects of drugs on voltage-dependent activation and fast inactivation of  $I_{Na}$ . Compared with the control group, BRV significantly shifted the potential for VGSCs half-inactivation ( $V_{50}$ ) to more hyperpolarized potentials at all three concentrations (1, 10 and 100  $\mu$ M) tested (Figure 1B, Table 1). CBZ shifted  $V_{50}$  for inactivation to more hyperpolarized values, at a concentration of 100  $\mu$ M, while 1 and 10  $\mu$ M did not induce a significant change in  $V_{50}$  (Figure 1B, Table 1). Neither BRV nor CBZ modified the voltage-dependent activation behavior of VGSCs (Table 1). To evaluate the channel state dependency on BRV and CBZ effects, we applied depolarizing pulses at a frequency of 1 Hz from potentials held at  $-120$  mV or at  $-80$  mV promoting the resting state or the inactivated state of VGSCs, respectively. From a holding potential at  $-120$  mV,  $I_{Na}$  was not modulated by any concentration of BRV or CBZ except by 1  $\mu$ M CBZ which produced a minor but significant decrease (<10%) of the current (Figure 1C). From a holding potential at  $-80$  mV,  $I_{Na}$  was significantly inhibited by BRV and CBZ at 1  $\mu$ M (~20%), 10  $\mu$ M (~25%), and 100  $\mu$ M (BRV: ~30%; CBZ: ~40%) (Figure 1C). These results show that  $I_{Na}$  blockade induced by BRV or CBZ was concentration- and inactivated channel state-dependent and that maximal  $I_{Na}$  inhibition was 10% lower with BRV than with CBZ.

### In Primary Cortical Neurons, BRV Reduces $I_{Na}$ but has no Effect on SRF

Effects of BRV and CBZ were tested on  $I_{Na}$  (Figure 2C–E) and on SRF (Figure 3) evoked in rat primary cortical neurons to compare our results with those previously reported from the same species [19].

In voltage-clamp, I–V curves recorded in primary cortical neurons (Figure 2A) showed a threshold of  $I_{Na}$  activation at  $-70$  mV,

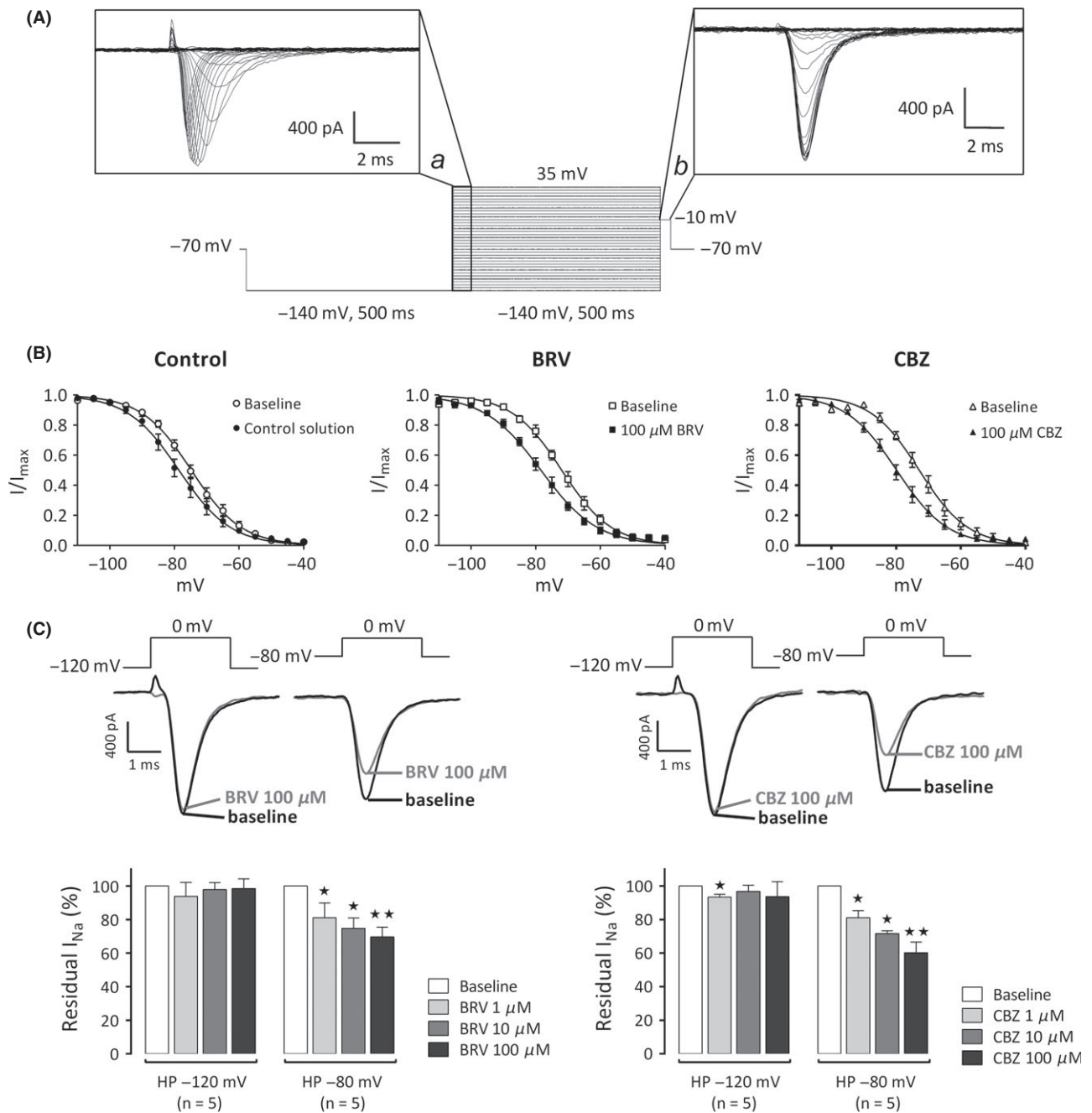


**Figure 1** Effect of brivaracetam (BRV) and carbamazepine (CBZ) on  $I_{Na}$  recorded in N1E-115 cells. **(A)** Stimulation protocol applied on N1E-115 cells to evaluate the effects of BRV (1–10–100  $\mu$ M) and CBZ (1–10–100  $\mu$ M) on activation (*a*) and fast inactivation (*b*) properties of  $I_{Na}$ . Traces in insets represent typical examples of  $I_{Na}$  recorded from resting state of VGSCs (*a*, left inset) and used to calculate  $I_{Na}$  activation curve, and of  $I_{Na}$  activated from preconditioning steps (*b*, right inset) and used to calculate  $I_{Na}$  fast inactivation curve. **(B)** Steady-state fast inactivation of  $I_{Na}$  obtained from "b" in the protocol described in **(A)** was evaluated under control conditions (Control,  $n = 5$ ), or in the presence of BRV ( $n = 5$ ), or CBZ ( $n = 5$ ). Graphs represent normalized  $I_{Na}$  activated at  $-10$  mV following preconditioning steps and measured before (open symbols) and after a 35-min perfusion with control solution or 100  $\mu$ M test drug (filled symbols). The results are expressed as mean  $\pm$  SEM. The mean values were fitted (lines) with a Boltzmann function. The potentials for half-inactivation ( $V_{50}$ ) were calculated on individual cells and then averaged. **(C)** To evaluate VGSC state dependency of  $I_{Na}$  inhibition induced by BRV and CBZ,  $I_{Na}$  was activated by 20 ms depolarizing pulses applied at 1 Hz from a holding potential at  $-120$  mV (resting state) or  $-80$  mV (corresponding to  $V_{50}$  of inactivation). Insets show representative traces of  $I_{Na}$  activated from  $-120$  mV and from  $-80$  mV, before (in black) and after 100  $\mu$ M drug (in gray) perfusion. Bars represent mean percentages ( $\pm$ SD) of residual  $I_{Na}$  normalized to predrug  $I_{Na}$  (baseline) for the number  $n$  of neurons. Significant differences versus baseline value are indicated with \*\* ( $P < 0.01$ ) and \* ( $P < 0.05$ ) using paired two-tailed *t*-test.



**Table 1** Cumulative dose–response effects of BRV and CBZ on the voltage dependence of  $I_{Na}$  activation and fast inactivation in N1E-115 cells

	Baseline $V_{50}$ (mV)	$\Delta V_{50}$ (mV) T1	$\Delta V_{50}$ (mV) T2	$\Delta V_{50}$ (mV) T3
Control (n = 5)				
Inactivation	$-74.9 \pm 3.0$	$-0.5 \pm 0.6$	$-1.2 \pm 0.9^*$	$-4.0 \pm 1.5^{**}$
Activation	$-30.2 \pm 1.8$	$-1.0 \pm 0.9$	$-0.9 \pm 1.5$	$-0.2 \pm 0.5$
BRV (n = 5)		1 $\mu$ M	10 $\mu$ M	100 $\mu$ M
Inactivation	$-71.8 \pm 3.2$	$-3.1 \pm 1.2^{**}$	$-4.8 \pm 0.8^{***}$	$-7.0 \pm 0.9^{**}$
Activation	$-25.8 \pm 2.5$	$-0.9 \pm 1.5$	$-1.5 \pm 1.7$	$-2.7 \pm 2.2$
CBZ (n = 5)		1 $\mu$ M	10 $\mu$ M	100 $\mu$ M
Inactivation	$-72.4 \pm 3.0$	$-1.1 \pm 0.9$	$-2.6 \pm 1.4$	$-7.9 \pm 1.9^{**}$
Activation	$-25.4 \pm 2.5$	$-0.2 \pm 0.5$	$-2.0 \pm 1.0$	$-3.2 \pm 1.9$

BRV, brivaracetam; CBZ, carbamazepine. Values are mean  $\pm$  SD and represent  $V_{50}$  or  $\Delta V_{50}$  ( $V_{50}$  at time Tx –  $V_{50}$  baseline).  $V_{50}$  values were measured from the fitted  $I_{Na}$  inactivation curves illustrated in Figure 1B and from the fitted activation curves (data not illustrated). Activation and inactivation curves were built before (baseline) and after 10 min perfusion of drugs applied at increasing concentrations (1  $\mu$ M, 10  $\mu$ M and 100  $\mu$ M) successively or after time-matched periods (T1 = 10 min, T2 = 20 min and T3 = 30 min) in control conditions. The number of neurons (n) per group is indicated between brackets. No difference was found in  $V_{50}$  values recorded at baseline in all groups of neurons. At T2 and T3,  $V_{50}$  values in control group showed significant differences (two-tailed *t*-test vs. baseline; \* $P < 0.05$ ; \*\* $P < 0.01$ ) indicating a time-dependent leftward shift of  $I_{Na}$  inactivation voltage dependency. Comparison between drug-treated groups and the control group was assessed on  $\Delta V_{50}$  values (two-tailed *t*-test; \*\* $P < 0.01$ ; \*\*\* $P < 0.001$ ).

a peak current at  $-30$  mV and a reversal potential around  $+50$  mV (calculated equilibrium potential for  $Na^+ = +42$  mV in 15 mM NaCl internally and 80 mM NaCl externally) confirming the  $Na^+$  nature of the recorded current. As the data obtained in N1E-115, cells showed that neither BRV nor CBZ were effective on  $I_{Na}$  activated from the resting state of VGSCs, we decided to test their effects in cortical neurons on  $I_{Na}$  activated only from  $V_{50}$  for inactivation. The voltage dependence of  $I_{Na}$  inactivation was investigated in each neuron before application of the drugs (Figure 2B). Fitted fast inactivation curves displayed similar  $V_{50}$  in the 3 groups of neurons before drug application (control group:  $-73.6$  mV  $\pm$  1.5 mV, mean  $\pm$  SD, n = 7; BRV group:  $-71.9$  mV  $\pm$  1.2 mV, n = 8, LSD test vs. control group  $P = 0.5456$ ; CBZ group:  $-74.4$  mV  $\pm$  2.5 mV, n = 4, LSD test vs. control group  $P = 0.7435$ ; ANOVA  $P = 0.6180$ ). BRV (300  $\mu$ M) and CBZ (100  $\mu$ M) were tested on  $I_{Na}$  activated by pulses applied at 0.1 Hz from  $V_{50}$  values for  $I_{Na}$  inactivation (Figure 2C–E). The drug was applied after a 5-min baseline period, and its effect on  $I_{Na}$  was evaluated at 400 seconds (Figure 2C,D), using a linear biregression fitting. Under control conditions, there was a linear run-down of  $I_{Na}$  amplitudes and which was not significantly altered by the application of the control solution (5%  $\pm$  6%, mean  $\pm$  SD) (Figure 2E). BRV and CBZ produced a significant decrease of  $I_{Na}$  by 27%  $\pm$  9% and 52%  $\pm$  6%, respectively (Figure 2E).  $I_{Na}$  inhibition was significantly higher with CBZ than BRV.

Sustained repetitive firing in primary cortical neurons (Figure 3A) was induced with a stimulation intensity ranging from 60 pA to 400 pA (153  $\pm$  77 pA, mean  $\pm$  SEM; 24 neurons). The stimulation intensity was individually selected to induce the highest tonic firing of APs without accommodation from a membrane potential held at  $-71$  mV  $\pm$  1 mV (24 neurons). In control conditions, SRF frequency was 10  $\pm$  4 Hz (mean  $\pm$  SEM; 24 neurons). As illustrated in Figure 3B, a 15-min perfusion of BRV did not modify the number of APs normalized to predrug value (96%  $\pm$  43%, mean  $\pm$  SD), similarly to a time-matched per-

fusion of control solution (89%  $\pm$  17%), while a time-matched perfusion of CBZ significantly reduced it to 13%  $\pm$  19% without abolishing the initial APs evoked at the onset of the step in half of the recorded neurons (3/6 neurons). The amplitude of the first AP elicited during SRF was not modified by the 15-min perfusion of control solution (baseline: 97 mV  $\pm$  4 mV, mean  $\pm$  SEM, n = 9; after 15 min: 98 mV  $\pm$  4 mV, n = 9; *t*-test  $P = 0.3883$ ), or after application of BRV (baseline: 96 mV  $\pm$  2 mV, n = 9; after 15 min: 96 mV  $\pm$  3 mV, n = 9; *t*-test  $P = 0.9466$ ), or CBZ in the three neurons continuing to fire (baseline: 92 mV  $\pm$  5 mV; after 15 min: 95 mV  $\pm$  5 mV, n = 3; *t*-test  $P = 0.8773$ ). The average of action potential amplitudes elicited in the same train (AP#3 to AP#15), normalized with baseline values, was not modified by the 15-min perfusion of control solution (100%  $\pm$  5%, mean  $\pm$  SD, n = 9) or BRV (93%  $\pm$  13%, n = 9; LSD test vs. control group  $P = 0.1072$ , ANOVA 0.0630) but was significantly reduced in the three CBZ-treated neurons continuing to fire (85%  $\pm$  1%, n = 3, LSD test vs. control group  $P = 0.0290$ ).

### In CA1 Pyramidal Neurons from Mouse Hippocampal Slices, BRV has no Effect on $I_{Na}$ and Does not Inhibit the SRF

Brivaracetam was previously reported to have potent anticonvulsant activity in a number of mouse epilepsy models [10], and we, therefore, decided to further investigate the effects of BRV and CBZ on  $I_{Na}$  (Figure 4) and SRF (Figure 5) in CA1 pyramidal neurons from mouse hippocampal slices.

In voltage-clamp, I–V curves recorded in CA1 neurons (Figure 4A) showed a threshold of  $I_{Na}$  activation around  $-70$  mV, a peak current between  $-30$  mV and  $-20$  mV, and a reversal potential around  $+50$  mV (calculated equilibrium potential for  $Na^+ = +37$  mV for 15 mM NaCl internally and 63 mM NaCl externally) confirming the  $Na^+$  nature of the recorded current. BRV and CBZ effects were evaluated on  $I_{Na}$  activated from  $V_{50}$

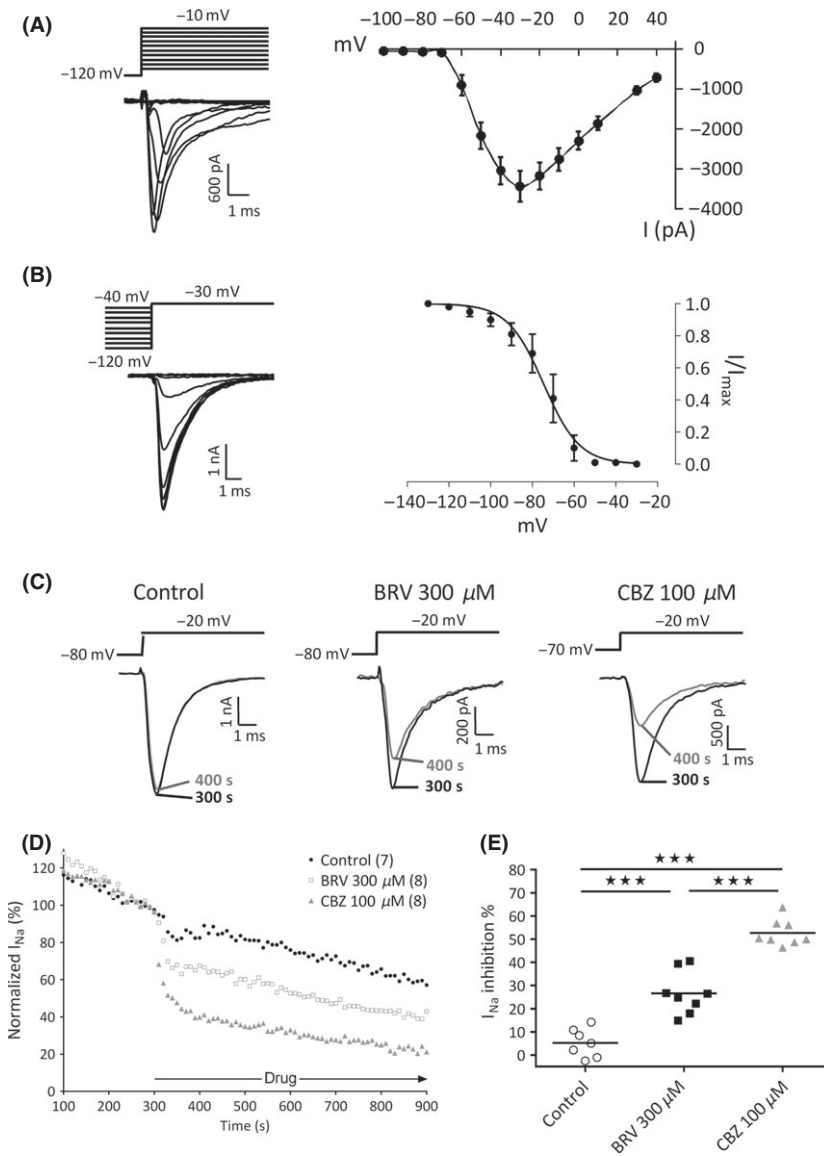


**Figure 2** Effect of brivaracetam (BRV) and carbamazepine (CBZ) on  $I_{Na}$  recorded in rat primary cortical neurons. **(A)** Mean  $I-V$  curve of  $I_{Na}$  recorded from a holding potential of  $-120$  mV before application of the drugs. Data represent mean  $\pm$  SEM for 19 neurons. Extrapolation of the curve indicates a reversal potential of the current around  $+50$  mV. Representative  $I_{Na}$  traces recorded from the protocol used to assess activation properties of  $I_{Na}$  are illustrated on the left. **(B)** Mean  $I_{Na}$  fast inactivation curve normalized to maximal  $I_{Na}$  recorded before application of the drugs. Data represent mean  $\pm$  SD for 19 neurons. Representative  $I_{Na}$  traces recorded from the protocol used to assess fast inactivation properties of  $I_{Na}$  are illustrated on the left. **(C)** Representative currents elicited by a depolarizing step at  $-20$  mV from the inactivation  $V_{50}$  of the recorded neurons. Superimposed traces represent currents before (300 seconds in black) and after 100-second perfusion (400 seconds in gray) with control solution, BRV, or CBZ. **(D)** Time course of  $I_{Na}$  activated at  $0.1$  Hz under control conditions (100–300 seconds) and during perfusion with control ( $n = 7$ ),  $300 \mu\text{M}$  BRV ( $n = 8$ ), and  $100 \mu\text{M}$  CBZ ( $n = 4$ ) (300–900 seconds). Symbols represent the mean. **(E)** Percentage of  $I_{Na}$  inhibition for control, BRV and CBZ groups measured using a linear biregression fitting (see Materials and Methods) of the curves illustrated in **(D)**. Symbols represent individual values and means are indicated with horizontal bars within groups. Significant differences in  $I_{Na}$  inhibition values (ANOVA and post hoc LSD test: \*\*\* $P < 0.001$ ) were found between both drug groups and the control group and between BRV group and CBZ group.

potential for inactivation. The voltage dependence of  $I_{Na}$  inactivation was investigated in each neuron before application of the drugs (Figure 4B). Fitted fast inactivation curves displayed similar  $V_{50}$  in the three groups of neurons (control group:  $-71.2$  mV  $\pm$   $3.1$  mV, mean  $\pm$  SEM,  $n = 5$ ; BRV group:  $-71.7$  mV  $\pm$   $3.2$  mV,  $n = 7$ , LSD test vs. control group  $P = 0.9284$ ; CBZ group:  $-69.8$  mV  $\pm$   $6.8$  mV,  $n = 4$ , LSD test vs. control group  $P = 0.8251$ ; ANOVA  $P = 0.9475$ ). BRV ( $300 \mu\text{M}$ ) and CBZ ( $100 \mu\text{M}$ ) were tested on  $I_{Na}$  activated by pulses applied at  $0.1$  Hz (Figure 4C–E). Under control conditions, we observed a linear rundown of  $I_{Na}$  amplitudes (Figure 4D). Thus, we evaluated the effects of drugs on  $I_{Na}$  using a linear biregression fitting. Control group showed a  $I_{Na}$  decrease of  $6\% \pm 3\%$  (mean  $\pm$  SEM) which was not different from the  $I_{Na}$  decrease measured in BRV group ( $5\% \pm 5\%$ ) (Figure 4E). By contrast, CBZ produced an inhibition of  $I_{Na}$  ( $42\% \pm 2\%$ ) which was statistically different from the values measured in control and BRV groups (Figure 4E).

Sustained repetitive firing in CA1 pyramidal neurons was induced by repetitive series of increasing depolarizing current steps applied every 10 min from a membrane potential held at  $-60$  mV (Figure 5). One-hour perfusion with either control solution or  $100 \mu\text{M}$  BRV did not significantly modify the number of APs for all step intensities, while a perfusion of 20 min with  $100 \mu\text{M}$  CBZ reduced the SRF evoked by step intensities ranging from  $300$  pA to  $500$  pA (Figure 5B). The effect of CBZ was maximal after 40 min of continuous perfusion. Figure 5C illustrates the time course of AP numbers evoked by  $400$  pA step normalized to predrug value in each group of neurons. In the control group and in the BRV group, the normalized APs number after 40 min was not significantly increased to  $119\% \pm 20\%$  (mean  $\pm$  SEM) (paired two-tailed  $t$ -test,  $P = 0.3847$ ), and  $126\% \pm 15\%$  ( $P = 0.1209$ ), respectively. By contrast, a time-matched perfusion with CBZ significantly reduced the AP number percentage to  $26\% \pm 7\%$  ( $P = 0.00005$ ). Similarly to the

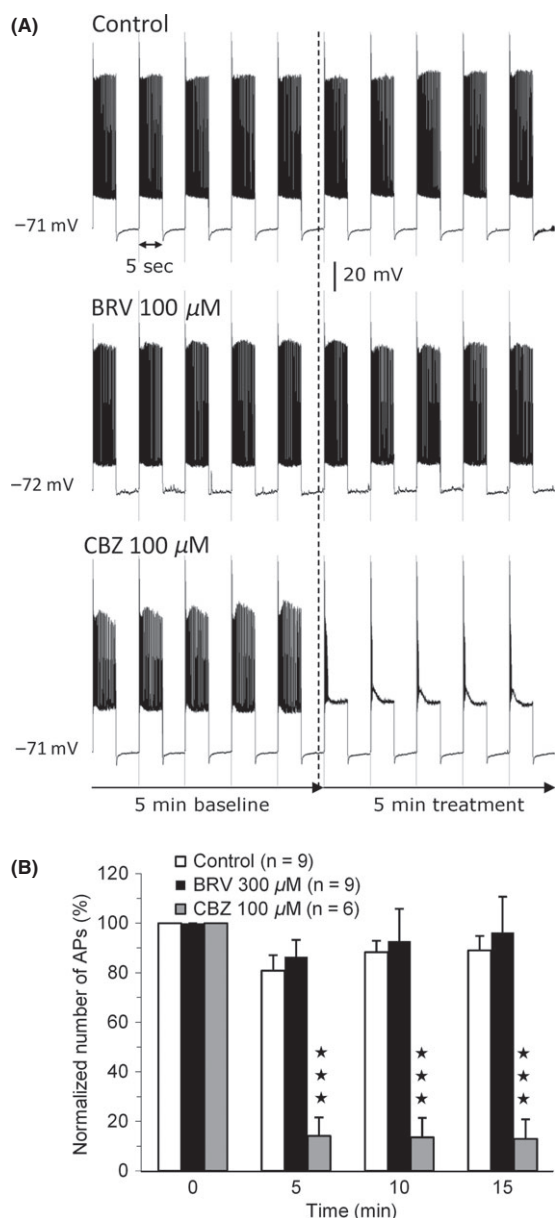


**Figure 3** Effect of brivaracetam (BRV) and carbamazepine (CBZ) on sustained repetitive firing (SRF) recorded in rat primary cortical neurons. **(A)** Traces represent concatenate display of SRFs recorded for 5 min (baseline) before and 5 min during application of either control solution or 300  $\mu$ M BRV or 100  $\mu$ M CBZ in different primary cortical neurons. SRF was evoked by repetitive 5-second depolarizing current steps with stimulation intensity adapted for each neuron (control neuron,  $I = 150$  pA; CBZ neuron,  $I = 70$  pA; BRV neuron,  $I = 250$  pA) and applied every minute from the resting membrane potential of the neurons (indicated at the left of each trace). The vertical dashed line corresponds to the onset of drug perfusion. **(B)** Graph represents the time course of the normalized number of action potential (APs) per step recorded during 15-min perfusion with control solution or with the drug. Normalization was performed with the number of APs elicited by the last step recorded during baseline. Bars are mean + SEM for the number of neurons  $n$ . Statistical differences between CBZ group and control group are indicated with  $***P < 0.001$  (unpaired two-tailed  $t$ -test).

SRF experiment performed in primary cortical neurons, initial APs evoked at the onset of the step were preserved during the perfusion with CBZ.

## Discussion

The aim of this study was to further explore the pharmacology of BRV on VGSCs expressed in different cell systems and to evaluate whether the effects of BRV on  $I_{Na}$  contribute to the regulation of neuronal excitability *in vitro*. The main findings were that BRV inhibits  $I_{Na}$  in mouse neuroblastoma cells and in rat primary cortical cultures, but not in CA1 pyramidal neurons from adult mice and does not reduce SRF induced in native or cultured neurons. In contrast, CBZ significantly reduced  $I_{Na}$  and SRF in all experiments and validated that the experimental conditions were sensitive to this standard AED known to block VGSCs.

Brivaracetam induced a minor but significant decrease of  $I_{Na}$  in the mouse N1E-115 neuroblastoma cell line and in cultured rat cortical neurons by modulating the fast-inactivated state of the channel, similar to CBZ, suggesting that BRV may act as a classical  $I_{Na}$  blocker. This corroborates a previous report [19], although the overall efficacy of BRV on inactivated VGSCs was much smaller in the present study (20–30% vs. 60%). A major difference between the two studies is the lack of effect of BRV on the resting state of VGSCs in our experimental conditions (Table 1) confirmed by the lack of change in the I-V relationship of  $I_{Na}$  recorded before and after application of 1, 10, or 100  $\mu$ M BRV or CBZ [25]. This discrepancy with the previous study [19] could be explained by the use of different experimental protocols. An overestimation of the BRV-induced  $I_{Na}$  inhibition could be due to the absence of a time-matched control group to correctly evaluate rundown of  $I_{Na}$ . Another possibility is that the effect of BRV would depend on neuronal maturation (8–12 DIV neurons in previous study vs. 9–19 DIV neurons in present study), and our data on mature CA1 neurons further support this hypothesis.

We have extended our investigations to hippocampal neurons from adult mice to evaluate the effects of BRV on  $I_{Na}$  activated in native mature neurons. Unexpectedly, BRV did not affect  $I_{Na}$  recorded in CA1 neurons from mouse hippocampal slices although CBZ induced a 42%  $I_{Na}$  inhibition under the same experimental conditions. This lack of effect in CA1 neurons was unexpected as a concentration of 100  $\mu$ M BRV was sufficient to produce a significant inhibition of  $I_{Na}$  in neuroblastoma cells (~30%, Figure 1C) and in cultured cortical neurons (~27%, Figure 2E) [19]. Several hypotheses can be advanced to explain the lack of effect of BRV in CA1 neurons. One reason could be that the VGSC isoforms expressed in each cell system may differ and that BRV would act preferentially on specific isoform(s) of VGSC. BRV effect might also differ due to the state of maturation of the cell systems used in this study. Neuroblastoma cells and primary cortical neurons did not undergo the full developmental changes and might differ in their physiology compared with neurons from adult brain. N1E-115 cells or primary cortical cultures are widely used to study the pharmacology of VGSC blockers [18–21,24,26–29] and although they express a mix of relevant VGSC isoforms [24], the absence or the presence of specific accessory proteins, the different metabolic state of VGSC (e.g., glycosylation, phosphory-

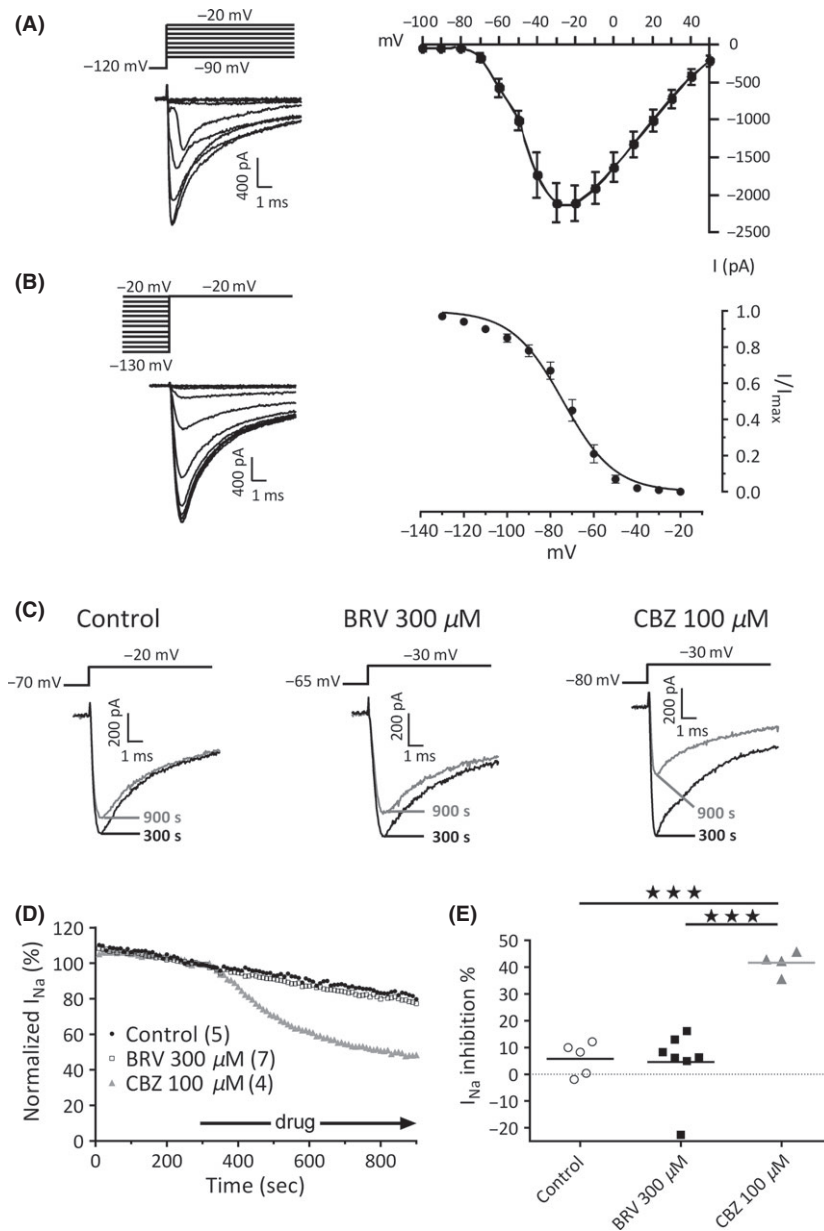


**Figure 4** Effect of brivaracetam (BRV) and carbamazepine (CBZ) on  $I_{Na}$  recorded in CA1 neurons from mouse hippocampal slices. **(A)** Mean  $I-V$  curve of  $I_{Na}$  recorded before application of the drugs. Data represent mean  $\pm$  SD for 16 neurons. Extrapolation of the curve indicates a reversal potential of the current around +50 mV. Representative series of  $I_{Na}$  traces recorded from the protocol are illustrated on the left. **(B)**  $I_{Na}$  fast inactivation curve normalized to maximal  $I_{Na}$  recorded before application of the drugs. Data represent mean  $\pm$  SEM for 16 neurons. Representative series of  $I_{Na}$  traces recorded from the protocol are illustrated on the left. **(C)** Representative currents elicited by a depolarizing step inducing peak  $I_{Na}$  from  $V_{50}$  value for  $I_{Na}$  inactivation adapted for each neuron. Superimposed traces represent currents before (300 seconds in black) and after 600-second perfusion (900 seconds in gray) with control, BRV, or CBZ. **(D)** Time course of  $I_{Na}$  activated at 0.1 Hz under control conditions (0–300 seconds) and during perfusion with control, 300  $\mu$ M BRV, and 100  $\mu$ M CBZ (300–900 seconds). Symbols represent the mean value for the number of neurons (n). **(E)** Percentage of  $I_{Na}$  inhibition for control, BRV, and CBZ groups measured using a linear biregression fitting (see Methods) of the curves illustrated in (D). Symbols represent individual values and means are indicated with horizontal bars within groups. Significant differences between CBZ group and control group and between BRV group and control group are indicated with \*\*\* ( $P < 0.001$ , ANOVA and post hoc LSD test).

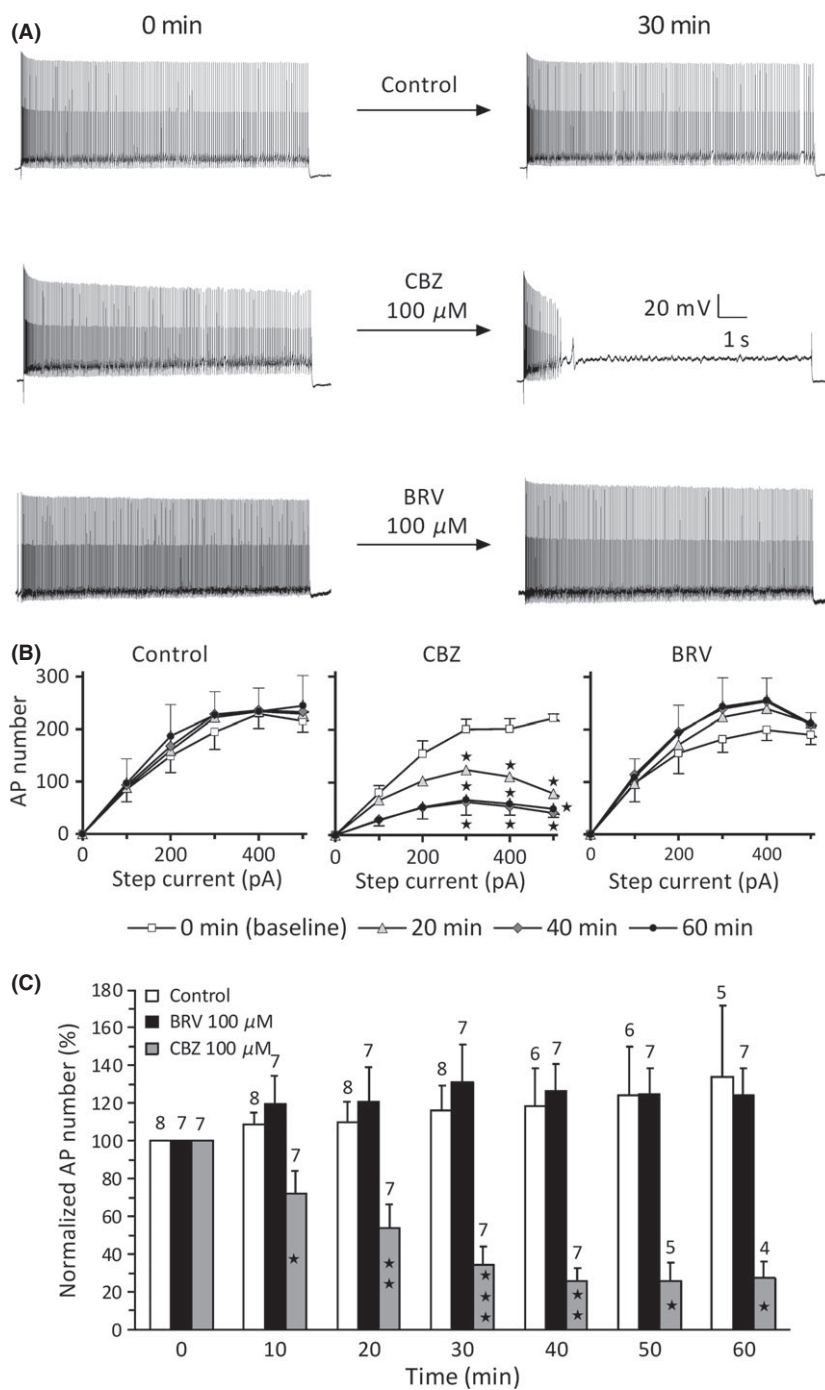
lation) or their localization may impact their responses to drugs. Although CBZ produces consistent inhibitory effects on  $I_{Na}$  in all cell systems tested in this study, the effects of BRV on  $I_{Na}$  remain quite small and such marginal effects may be strongly affected by the cellular background. Similar observations have been recently made with cannabinoids compounds which produced strong inhibition of  $I_{Na}$  in recombinant cell lines or neuronal culture system but with minimal or no effect in mature neurons [30].

The lack of effect of BRV on  $I_{Na}$  in adult CA1 neurons correlates with its absence of effect on SRF induced in these neurons. Evoked SRF is used to mimic a hyperexcitable state of neurons leading to an increase of neurotransmitter release as it occurs during interictal or ictal discharges [23]. CBZ and other AEDs with an anticonvulsant mechanism mediated by the blockade of VGSCs are reported to reduce SRF [27,31–35]. The lack of effect of BRV

on SRF suggests, therefore, that its antiepileptic mechanism would be unrelated to a blockade of VGSCs. Preliminary studies obtained in our laboratory with BRV (300  $\mu$ M) in entorhinal cortex neurons from adult mice did also not reveal a significant inhibition of  $I_{Na}$  or SRF (data not shown). BRV produced  $\sim$ 27% inhibition of  $I_{Na}$  in cultured cortical neurons which did not translate into an inhibition of SRF (Figure 3). CBZ which inhibited  $I_{Na}$  by  $\sim$ 52% under the same experimental conditions, reduced the AP firing frequency by more than 85% suggesting that the weak efficacy of BRV at reducing  $I_{Na}$  in these neurons is not sufficient to inhibit SRF. This hypothesis was supported by the analysis of AP amplitude during the SRF which detected a small nonsignificant reduction of 7% in APs amplitude average (AP#3 to AP#15) in BRV group, while CBZ perfusion significantly reduced the amplitude of APs before abolishing AP firing (data not shown).



**Figure 5** Effect of brivaracetam (BRV) and carbamazepine (CBZ) on sustained repetitive firing (SRF) evoked in CA1 neurons from mouse hippocampal slices. **(A)** Representative traces of SRF recorded before (0 min) and after 30 min treatment with either control solution, 100  $\mu$ M CBZ or 100  $\mu$ M BRV in three different CA1 hippocampal neurons. SRF was induced by a 10 seconds depolarizing current step (step current intensity for the displayed examples: 300 pA) applied from a potential held at  $-60$  mV. **(B)** Graphs represent the number of action potential (APs) elicited per series of increasing depolarizing steps recorded at different time points before (0 min = baseline) and after perfusion (20 min, 40 min and 60 min) with control solution ( $n = 5-8$  neurons), 100  $\mu$ M BRV ( $n = 7$  neurons), and 100  $\mu$ M CBZ ( $n = 4-7$  neurons). The number of APs according to stimulation intensity in control group and in BRV group was not different from their respective baseline curve. In the CBZ group, the number of APs was significantly reduced compared to the baseline curve (paired two-tailed *t*-test:  $*P < 0.05$ ) after 20 min perfusion with the drug and this reduction was maximal after 40 min perfusion. Symbols and errors bars represent means and SEMs, respectively. **(C)** Bar graph represent normalized APs number induced by the 400 pA depolarizing step recorded at different time points after perfusion with control solution, 100  $\mu$ M BRV or 100  $\mu$ M CBZ. Number of APs was normalized to the number of APs elicited predrug (time 0). Values in the BRV group and in the control group were not different throughout the 60-min experiment. Comparison of values obtained in the CBZ group and in the control group showed significant differences (unpaired two-tailed *t*-test:  $*P < 0.05$ ;  $**P < 0.01$ ;  $***P < 0.001$ ) after a 10-min drug perfusion. Bars represent means + SEMs for the number of neurons indicated above error bars.



Brivaracetam, a close analog of levetiracetam, was developed as a second generation SV2A ligand with improved binding properties to the SV2A protein. The SV2A binding affinities of BRV and LEV correlate to their efficacy in epilepsy models, suggesting that their anticonvulsant activity is mediated via the SV2A protein [9,10]. The roles and function of the SV2A protein have been abundantly studied but are still not fully elucidated. It was demonstrated that SV2A is involved in normal synaptic

vesicle function and would participate in synaptic vesicle cycling and neurotransmitter release (for review in [36]). LEV was demonstrated to act presynaptically by decreasing neurotransmitter release in an SV2A-dependent manner [37] and especially under conditions of sustained neuronal activity [12,13]. Similar observations have been made for BRV [38] further supporting the hypothesis that the mechanism of BRV is mediated via SV2A. Additionally, *in vitro* electrophysiological studies showed that

LEV and BRV are mainly active against hypersynchrony in neuronal network and not against intrinsic hyperexcitability [10,22,39] which is confirmed by the present data demonstrating that BRV is not efficient at reducing neuronal intrinsic excitability.

Overall, all current hypotheses point toward a common and predominant effect of BRV and LEV to reduce synaptic transmission and neuronal network synchrony in hyperexcitability conditions.

## Conclusion

A recent study in which BRV was shown to inhibit VGSCs in the inactivated and resting states [19] led us to hypothesize that BRV may reduce neuronal excitability by blocking high repetitive AP firing in neurons. Overall, our data do not validate this hypothesis and suggest that the antiepileptic properties of BRV do not involve a change in sustained repetitive firing mediated by a blockade of

VGSCs. The main molecular mechanism of action described for BRV is related to its high-affinity binding to the SV2A protein [9], by decreasing the release of neurotransmitter during high-frequency synaptic activity or during interictal or ictal discharges [10,38]. Taken together, these results further support that the antiepileptic properties of BRV are mediated through a selective, high-affinity binding to SV2A [9,10].

## Acknowledgments

We thank Michaëlla Grossman, Nathalie Pacico, and Nadine Noël for the preparation of primary cortical cultures and neuroblastoma cells.

## Conflict of Interest

All authors are employed by UCB Pharma, Belgium.

## References

- Kasteleijn-Nolst Trenite DG, Genton P, Parain D, et al. Evaluation of brivaracetam, a novel SV2A ligand, in the photosensitivity model. *Neurology* 2007;**69**: 1027–1034.
- Malawska B, Kulig K. Brivaracetam: A new drug in development for epilepsy and neuropathic pain. *Expert Opin Investig Drugs* 2008;**17**:361–369.
- Van Paesschen W, Hirsch E, Johnson M, Falter U, von Rosenstiel P. Efficacy and tolerability of adjunctive brivaracetam in adults with uncontrolled partial-onset seizures: A phase IIb, randomized, controlled trial. *Epilepsia* 2013;**54**:89–97.
- Kwan P, Trinka E, Van Paesschen W, Rektor I, Johnson ME, Lu S. Adjunctive brivaracetam for uncontrolled focal and generalized epilepsies: Results of a phase III, double-blind, randomized, placebo-controlled, flexible-dose trial. *Epilepsia* 2014;**55**:38–46.
- Ryvlin P, Werhahn KJ, Blaszczyk B, Johnson ME, Lu S. Adjunctive brivaracetam in adults with uncontrolled focal epilepsy: Results from a double-blind, randomized, placebo-controlled trial. *Epilepsia* 2014;**55**:47–56.
- Biton V, Berkovic SF, Abou-Khalil B, Sperling MR, Johnson ME, Lu S. Brivaracetam as adjunctive treatment for uncontrolled partial epilepsy in adults: A phase III randomized, double-blind, placebo-controlled trial. *Epilepsia* 2014;**55**:7–66.
- Rogawski MA. Brivaracetam: A rational drug discovery success story. *Br J Pharmacol* 2008;**154**:1555–1557.
- Lynch BA, Lambeng N, Nocka K, et al. The synaptic vesicle protein SV2A is the binding site for the antiepileptic drug levetiracetam. *Proc Natl Acad Sci USA* 2004;**101**:9861–9866.
- Gillard M, Fuks B, Leclercq K, Matagne A. Binding characteristics of brivaracetam, a selective, high affinity SV2A ligand in rat, mouse and human brain: Relationship to anti-convulsant properties. *Eur J Pharmacol* 2011;**664**:36–44.
- Matagne A, Margineanu DG, Kenda B, Michel P, Klitgaard H. Anti-convulsive and anti-epileptic properties of brivaracetam (ucb 34714), a high-affinity ligand for the synaptic vesicle protein, SV2A. *Br J Pharmacol* 2008;**154**:1662–1671.
- Sargentini-Maier ML, Rolan P, Connell J, et al. The pharmacokinetics, CNS pharmacodynamics and adverse event profile of brivaracetam after single increasing oral doses in healthy males. *Br J Clin Pharmacol* 2007;**63**:680–688.
- Yang XF, Weisenfeld A, Rothman SM. Prolonged exposure to levetiracetam reveals a presynaptic effect on neurotransmission. *Epilepsia* 2007;**48**:1861–1869.
- Meehan AL, Yang X, McAdams BD, Yuan L, Rothman SM. A new mechanism for antiepileptic drug action: Vesicular entry may mediate the effects of levetiracetam. *J Neurophysiol* 2011;**106**:1227–1239.
- Klitgaard H, Verdru P. Levetiracetam: The first SV2A ligand for the treatment of epilepsy. *Expert Opin Drug Discov* 2007;**2**:1537–1545.
- Niespodziany I, Klitgaard H, Margineanu DG. Levetiracetam inhibits the high-voltage-activated Ca(2+) current in pyramidal neurons of rat hippocampal slices. *Neurosci Lett* 2001;**306**:5–8.
- Vogl C, Mochida S, Wolff C, Whalley BJ, Stephens GJ. The synaptic vesicle glycoprotein 2A ligand levetiracetam inhibits presynaptic Ca2+ channels through an intracellular pathway. *Mol Pharmacol* 2012;**82**:199–208.
- Rigo JM, Hans G, Nguyen L, et al. The anti-epileptic drug levetiracetam reverses the inhibition by negative allosteric modulators of neuronal GABA- and glycine-gated currents. *Br J Pharmacol* 2002;**136**:659–672.
- Zona C, Niespodziany I, Marchetti C, Klitgaard H, Bernardi G, Margineanu DG. Levetiracetam does not modulate neuronal voltage-gated Na+ and T-type Ca2+ currents. *Seizure* 2001;**10**:279–286.
- Zona C, Pieri M, Carunchio I, Curcio L, Klitgaard H, Margineanu DG. Brivaracetam (ucb 34714) inhibits Na(+) current in rat cortical neurons in culture. *Epilepsy Res* 2010;**88**:46–54.
- Matsuki N, Quandt FN, Ten Eick RE, Yeh JZ. Characterization of the block of sodium channels by phenytoin in mouse neuroblastoma cells. *J Pharmacol Exp Ther* 1984;**228**:523–530.
- Willow M, Gono T, Catterall WA. Voltage clamp analysis of the inhibitory actions of diphenylhydantoin and carbamazepine on voltage-sensitive sodium channels in neuroblastoma cells. *Mol Pharmacol* 1985;**27**:549–558.
- Niespodziany I, Klitgaard H, Margineanu DG. Desynchronizing effect of levetiracetam on epileptiform responses in rat hippocampal slices. *NeuroReport* 2003;**14**:1273–1276.
- Rogawski MA, Loscher W. The neurobiology of antiepileptic drugs. *Nat Rev Neurosci* 2004;**5**:553–564.
- Niespodziany I, Leclere N, Vandemplas C, Foerch P, Wolff C. Comparative study of lacosamide and classical sodium channel blocking antiepileptic drugs on sodium channel slow inactivation. *J Neurosci Res* 2013;**91**:436–443.
- Niespodziany I, Leclère N, Matagne A, Wolff C. Brivaracetam modulates Na currents expressed in a neuroblastoma cell line: Comparison with carbamazepine. *Epilepsia* 2009;**50**(Suppl. 11):107. Abstract Number 1.217.
- Bonifacio MJ, Sheridan RD, Parada A, Cunha RA, Patmore L, Soares-da-Silva P. Interaction of the novel anticonvulsant, BIA 2-093, with voltage-gated sodium channels: Comparison with carbamazepine. *Epilepsia* 2001;**42**:600–608.
- Errington AC, Stohr T, Heers C, Lees G. The investigational anticonvulsant lacosamide selectively enhances slow inactivation of voltage-gated sodium channels. *Mol Pharmacol* 2008;**73**:157–169.
- Quandt FN. Modification of slow inactivation of single sodium channels by phenytoin in neuroblastoma cells. *Mol Pharmacol* 1988;**34**:557–565.
- Zona C, Siniscalchi A, Mercuri NB, Bernardi G. Riluzole interacts with voltage-activated sodium and potassium currents in cultured rat cortical neurons. *Neuroscience* 1998;**85**:931–938.
- Hill AJ, Jones NA, Smith I, et al. Voltage-gated sodium (NaV) channel blockade by plant cannabinoids does not confer anticonvulsant effects per se. *Neurosci Lett* 2014;**566**:269–274.
- Calabresi P, Centonze D, Marfia GA, Pisani A, Bernardi G. An in vitro electrophysiological study on the effects of phenytoin, lamotrigine and gabapentin on striatal neurons. *Br J Pharmacol* 1999;**126**:689–696.
- DeLorenzo RJ, Sombati S, Coulter DA. Effects of topiramate on sustained repetitive firing and spontaneous recurrent seizure discharges in cultured hippocampal neurons. *Epilepsia* 2000;**41**(Suppl 1):S40–S44.
- Deshpande LS, Nagarkatti N, Sombati S, DeLorenzo RJ. The novel antiepileptic drug carisbamate (RWJ 333369) is effective in inhibiting spontaneous recurrent seizure discharges and blocking sustained repetitive firing in cultured hippocampal neurons. *Epilepsy Res* 2008;**79**:158–165.
- McLean MJ, Macdonald RL. Carbamazepine and 10,11-epoxycarbamazepine produce use- and voltage-dependent limitation of rapidly firing action potentials of mouse central neurons in cell culture. *J Pharmacol Exp Ther* 1986;**238**:727–738.
- White HS, Wolf HH, Swinyard EA, Skeen GA, Sofia RD. A neuropharmacological evaluation of felbamate as a novel anticonvulsant. *Epilepsia* 1992;**33**:564–572.
- Mendoza-Torresblanca JG, Vanoye-Carlo A, Phillips-Farfan BV, Carmona-Aparicio L, Gomez-Lira G. Synaptic vesicle protein 2A: Basic facts and role in synaptic function. *Eur J Neurosci* 2013;**38**:3529–3539.

37. Nowack A, Malarkey EB, Yao J, Bleckert A, Hill J, Bajjalieh SM. Levetiracetam reverses synaptic deficits produced by overexpression of SV2A. *PLoS One* 2011;**6**: e29560.
38. Yang X, Rothman SM, Dubinsky J. Brivaracetam is superior to levetiracetam in decreasing excitatory synaptic transmission. *Epilepsia* 2013;**1**:207. Abstract.
39. Margineanu DG, Klitgaard H. Inhibition of neuronal hypersynchrony in vitro differentiates levetiracetam from classical antiepileptic drugs. *Pharmacol Res* 2000;**42**:281–285.

## Supporting Information

The following supplementary material is available for this article:

**Data S1.** Electrophysiological experiments performed in the different investigated cell systems.